PROCEEDINGS OF SPIE

SPIEDigitalLibrary.org/conference-proceedings-of-spie

An efficient stable optical polariser module for calibration of the S4UVN earth observation satellite

Stephen Rolt, Ariadna Calcines, Bartosz Lomanowski, David Bramall, Benjamin Shaw

Stephen Rolt, Ariadna Calcines, Bartosz Lomanowski, David Bramall, Benjamin Shaw, "An efficient stable optical polariser module for calibration of the S4UVN earth observation satellite," Proc. SPIE 9912, Advances in Optical and Mechanical Technologies for Telescopes and Instrumentation II, 99126V (22 July 2016); doi: 10.1117/12.2232358

SPIE.

Event: SPIE Astronomical Telescopes + Instrumentation, 2016, Edinburgh, United Kingdom

An Efficient Stable Optical Polariser Module for Calibration of the S4UVN Earth Observation Satellite

Stephen Rolt, Ariadna Calcines, Bartosz Lomanowski, David Bramall and Benjamin Shaw

Durham University, Centre for Advanced Instrumentation, William Armstrong Way, Sedgefield, County Durham, United Kingdom, TS21 3FH.

ABSTRACT

We describe here an optical polariser module intended to deliver well characterised polarised light to an imaging spectrometer instrument. The instrument in question is the Sentinel-4/UVN Earth observation imaging spectrometer due to be deployed in 2019 in a geostationary orbit. The polariser module described here will be used in the ground based calibration campaign for this instrument. One critical task of the calibration campaign will be the highly accurate characterisation of the polarisation sensitivity of instrument. The polariser module provides a constant, uniform source of linearly polarised light whose direction can be adjusted without changing the output level or uniformity of the illumination.

A critical requirement of the polariser module is that the illumination is uniform across the exit pupil. Unfortunately, a conventional Glan-Taylor arrangement cannot provide this uniformity due to the strong variation in transmission at a refractive surface for angles close to the critical angle. Therefore a modified prism arrangement is proposed and this is described in detail. Detailed tolerance modelling and straylight modelling is also reported here.

Keywords: Polarisation, birefringence, Glan-Taylor, prism, tolerancing, straylight.

1: INTRODUCTION

This article describes the design and modelling of a collimating telescope used to illuminate an imaging spectrometer with stable, well characterised polarised light in the ultra-violet, visible and near infra-red spectral regions. The spectrometer is the Sentinel 4-UVN Earth observation satellite instrument due to be deployed in 2019 in a geostationary orbit. This instrument is an imaging spectrometer whose ultimate purpose is to image the spectral irradiance of the Earth with a view to spectroscopically mapping atmospheric contaminants[1,2]. This paper deals specifically with an optical system, the polarising module, used in the ground based calibration of the Sentinel 4 instrument.

The purpose of the polarising module is to present collimated, polarised light to the 80 mm diameter instrument input pupil during the ground based calibration programme. The instrument itself is to be located within a thermal vacuum chamber and the polarising module placed outside. As a consequence of this arrangement, the instrument pupil is located a considerable distance (2500 mm) from the polarising module. However, this is not a significant issue in that the field of view of the module is small (4 arcminutes). More specifically, a small aperture located at the polariser focal plane is uniformly illuminated by a variety of sources and the polarising module collimates this light. For practical design purposes, this arrangement represents the collimation of what amounts to a point source.

Advances in Optical and Mechanical Technologies for Telescopes and Instrumentation II,
edited by Ramón Navarro, James H. Burge, Proc. of SPIE Vol. 9912, 99126V
 · doi: 10.1117/12.2232358

The instrument, and thus the polariser module, is designed to operate in two primary wavebands. Firstly the UV-VIS waveband from 305-500 nm and secondly an NIR band from 750-775 nm. Illumination is provided in two forms. Firstly, there is broadband continuum emission provided by a xenon arc lamp source and secondly there is widely tunable emission from a narrowband laser source. In operation, the instrument will accurately characterise the polarisation state of light scattered from the Earth's atmosphere. More specifically, the instrument will measure the polarisation dependence of the bi-directional scattering distribution function (BSDF). Since the instrument itself might be expected to contribute to the measured polarisation sensitivity, an important part of the calibration process is to calibrate out the background polarisation sensitivity of the instrument itself. This is the function of the polarisation module. For this calibration process to work effectively, a number of key requirements must be fulfilled in the design and assembly of the polarisation module:

i) Output irradiance should be uniform across the 80 mm diameter instrument pupil
ii) Output should be linearly polarised with a contrast ratio of greater than 500
iii) The direction of linear polarisation should be adjustable over 360°
iv) The direction of linear polarisation should be known absolutely to 6 arcminutes
v) The level of temporal stability of the output flux should be very high (up to 1 part in 10^4)
vi) The wavefront error of the module should be less than 150 nm rms

To understand the construction of the polarisation module and how it would be deployed during testing, a simplified schematic arrangement is shown in Figure 1.

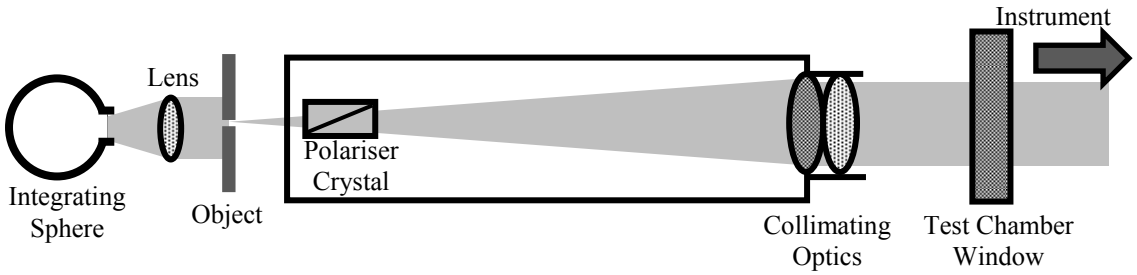

Figure 1: General schematic of polarisation module setup. The object is illuminated by output from an integrating sphere with the port aperture defining the input pupil and a lens interposed to provide telecentric illumination. Linear polarisation is effected by means of a polarisation crystal.

2 BASIC DESIGN CONSIDERATIONS

2.1 General

This article will be principally concerned with the design of the module 'downstream' from the object target. That said, illumination of the object via the integrating sphere, as shown in Figure 1 does define the input pupil and its location. The lens shown in Figure 1 ensures that the input pupil is located at infinity. Of course, the remainder of the optics should image the input pupil at the location of the instrument pupil – 2500 mm from the collimating optics. The integrating sphere, in turn, is illuminated by fibre feed either by a broadband xenon arc lamp source or by a tunable laser source. In order to stabilise the output flux level, illumination is monitored via a photodiode located in the integrating sphere and controlled by an active feedback mechanism.

Not only is the direction of linear polarisation to be swept through a full 360°, this should be done without affecting the temporal stability of the output. With this in mind, a transmissive collimator design seems the most appropriate choice.

That is to say, as illustrated in Figure 1, an entirely axial geometry can be adopted, including the polariser crystal. Rotation of this entire assembly would effect a rotation in the direction of linear polarisation without significantly changing the system throughput during this process. This throughput invariance would be difficult to achieve with an off-axis mirror system. On the other hand, the transmissive system will inevitably produce some chromatic aberration that would be absent from a mirror design. Overall, however, considerations of output stability prevail and an axial, transmissive system forms the basis of the module design.

As far as the collimating system is concerned, it must provide reasonably achromatic performance over the entire wavelength range from 305 – 775 nm. Whilst in the visible portion of the spectrum achromatic design is a relatively straightforward proposition, for the ultra-violet portion of the spectrum, materials choices are rather limited. In this instance, for practical purposes, we are restricted to a combination of fused silica and calcium fluoride lens materials. There is one other variable that can be controlled, namely the 'speed' of the collimator. From the point of view of the wavefront error, the 'slowest' possible design is preferred. However, for a fixed exit pupil size of 80 mm, increasing the f number of the design increases the module length and practical considerations limit module size. In this instance, an f#21 design was selected providing a compromise between size and performance.

2.2 Polarising Crystal

Figure 2 shows the geometry of a Glan-Taylor polarising crystal[3].

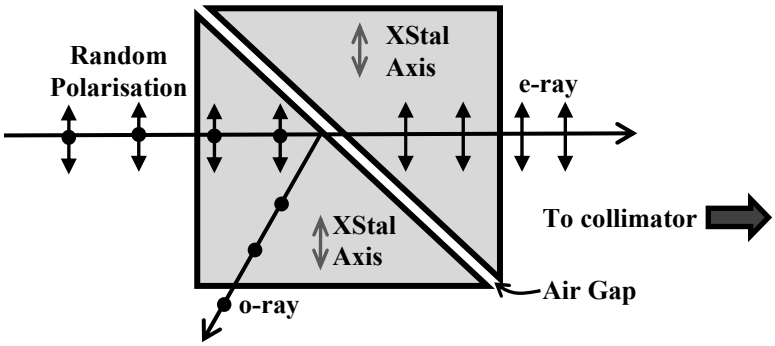

Figure 2 Conventional Glan-Taylor Polariser Geometry. Unpolarised light comes from the object to the left and polarised light emerges as the extra-ordinary ray. The ordinary ray is rejected by total internal reflection.

The Glan-Taylor polariser works by rejecting the ordinary polarised light by virtue of total internal reflection at the crystal-air interface whilst transmitting the extra-ordinary polarisation. This mechanism works in a birefringent crystal, such as calcite or barium borate, because of a significant difference in the refractive index between the two polarisations. That is to say, the critical angle is different for the two different polarisations. However, there is a relatively small 'window' of angles where the ordinary ray is rejected and the extra-ordinary ray transmitted. Therefore, it is only possible for the crystal to accommodate a small range (a few degrees) of incident angles. This further limits the module aperture.

Whilst total internal reflection provides complete rejection of the ordinary ray, the extra-ordinary ray is not wholly transmitted; there is residual Fresnel reflection. This reflection becomes more significant as the incident angle approaches the critical angle. It is clear that the transmission of the extra-ordinary ray has a strong dependence on the angle and thus the pupil position. This provides an extra-justification for keeping the system aperture as small as possible. Figure 3 illustrates this point by plotting the critical angle for internal reflection versus wavelength in barium borate with the angle referenced to an axis arranged at 38° to the interface normal.

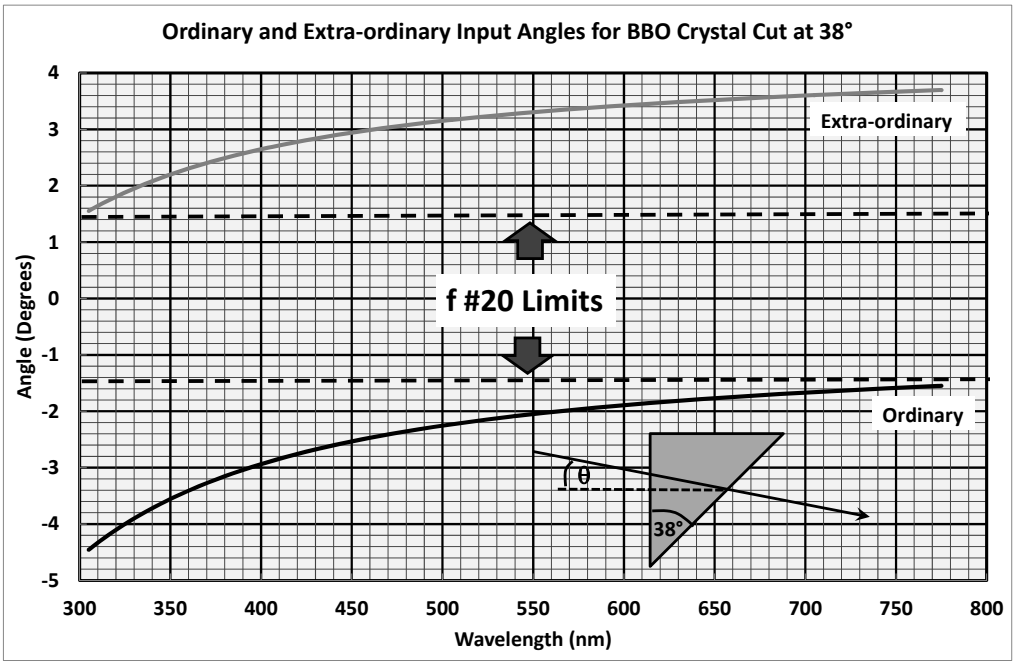

Figure 3: Ordinary and extraordinary internal reflection angles for a barium borate crystal. The angles are referenced to an axis at 38° to the surface normal. Practical working limits for f#20 illumination are also shown.

Figure 3 does not tell the whole picture as the extra-ordinary ray suffers significant angle dependent Fresnel reflection leading to non-uniform illumination of the pupil. Variation in irradiance across the f#20 pupil would be greater than 40% because of the varying Fresnel losses. For a single Glan-Taylor polarising crystal, this variation would present itself as a monotonic variation in irradiance from one end of the pupil to the other. Essentially the problem presents itself as a pseudo-linear dependence of transmission as a function of angle and hence pupil position. Consequentially, the issue may be ameliorated by introducing an additional polarising prism with the opposing symmetry. This, of course, comes at the cost of a slight reduction in throughput. The scheme is illustrated in Figure 4.

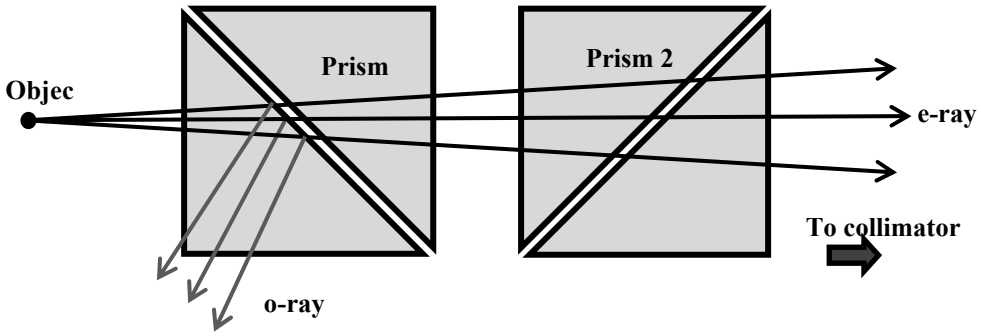

Figure 4: Double prism arrangement. Note the difference in symmetry between the two prisms.

Use of the double prism arrangement does not entirely eliminate the pupil non-uniformity. Angle dependent Fresnel losses in the extra-ordinary ray are now symmetrical about the chief ray, rather than displaying a monotonic variation.

2.3 Beam Telescope

Achieving the required wavefront error of less than 150 nm rms necessitates the use of an achromatic design. In many respects, the design is not challenging as the collimation optics are very slow at f#21. In the light of preceding

arguments, and the case for a transmissive design, a simple achromatic doublet should suffice. However, the choice of lens materials is rather limited on account of the wavelength range of the instrument. Good transmission at 305 nm entirely precludes the choice of glass materials and fused silica and calcium fluoride are the only practical options in this instance. Of course, conventional, visible oriented Abbe numbers are not appropriate to describe the dispersion of these materials. Instead, we use a 'special purpose' Abbe number, V_{S4}, where the three wavelengths used are 305, 400 and 775 nm. In line with this argument, the relevant Abbe number and partial dispersion, P_{S4}, is given by:

$$V_{S4} = \frac{n_{400} - 1}{n_{305} - n_{775}} \quad P_{S4} = \frac{n_{400} - n_{775}}{n_{305} - n_{775}} \tag{1}$$

By these definitions, the relevant Abbe numbers and partial dispersions are as given in Table 1.

Table 1: Dispersion parameters for Fused Silica and Calcium Fluoride for the S4 UVN Instrument wavelength range.

Material	**Fused Silica**	**Calcium Fluoride**
Abbe Number	14.39	19.83
Partial Dispersion	0.501	0.496

These Abbe numbers are rather smaller than one might expect from values pertaining to the classical visible range. However, the wide S4 UVN wavelength range produces greater refractive index differences. In addition, the contrast in the two Abbe numbers is not great, implying that the negative 'flint' element, i.e. calcium fluoride, needs to have a substantial diverging power. For an aperture of f#21 and an aperture of 80 mm, the system focal length needs to be 1680 mm. Although, ultimately, the system optimisation is rather more complex, this gives useful initial 'trial' values for the two lens focal lengths:

Fused Silica: f = 460 mm; Calcium Fluoride: f = -634 mm

Some secondary colour will be evident, given the difference in partial dispersion. The additional design freedom provided by the lens shape should be sufficient to correct for spherical aberration.

2.4 Location of exit pupil

Illumination of the small object target is telecentric. There is an additional constraint imposed by the desired location of the exit pupil – 2500 mm from the far end of the polarisation module. Therefore an additional small singlet lens needs to be placed between the polarising crystal and doublet collimating lens to provide the correct pupil location.

3: SYSTEM DESIGN

3.1 General Layout

Figure 5 shows the general system layout.

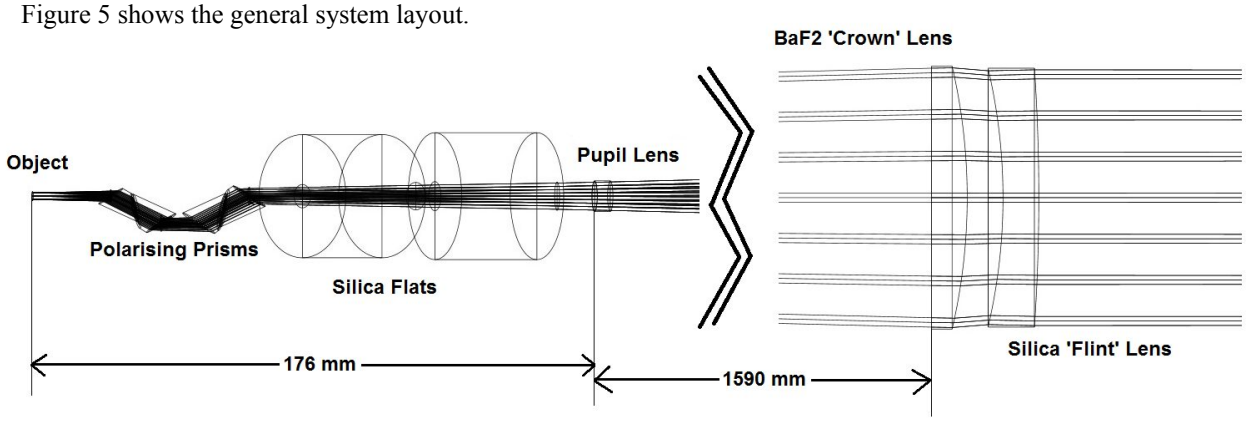

Figure 5: General system layout. The ray trace shows the crystal, pupil relay lenses and collimating lens in addition to other components.

The layout shown in Figure 5 introduces a number of new features absent from the idealised description in Figure 1. Firstly, as explained previously, a modified Glan-Taylor prism arrangement is used as the polariser. This incorporates two sets of prisms, rather than one, in order to improve the pupil uniformity. As will be outlined later, the polarising prisms are to be further modified such that the incident angle of the chief ray is at the Brewster angle (for the extra-ordinary ray) rather than normal. This effective tilt introduces additional astigmatism into the design which is corrected by means of two 45° tilted silica flats which produce countervailing astigmatism. In addition, a simple plano-convex fused silica lens, located close to the polarising crystals, provides correct imaging for the exit pupil.

3.2 Polarising Prisms

For reasons highlighted earlier, the polariser is to be implemented as a double Glan-Taylor type arrangement. However, the classical Glan-Taylor arrangement also introduces image ghosts from reflection of the front and rear facets. For a variety of reasons, in this application, it is not possible to ameliorate this ghosting by the application of anti-reflection coatings to moderate the Fresnel reflections. Therefore, a novel, modified arrangement is proposed. To avoid ghost reflections from front and rear facets of the prism, each prism is specially cut such that both facets are presented at the Brewster angle to the extra-ordinary ray. A magnified ray trace diagram is shown in Figure 6 and highlights this arrangement.

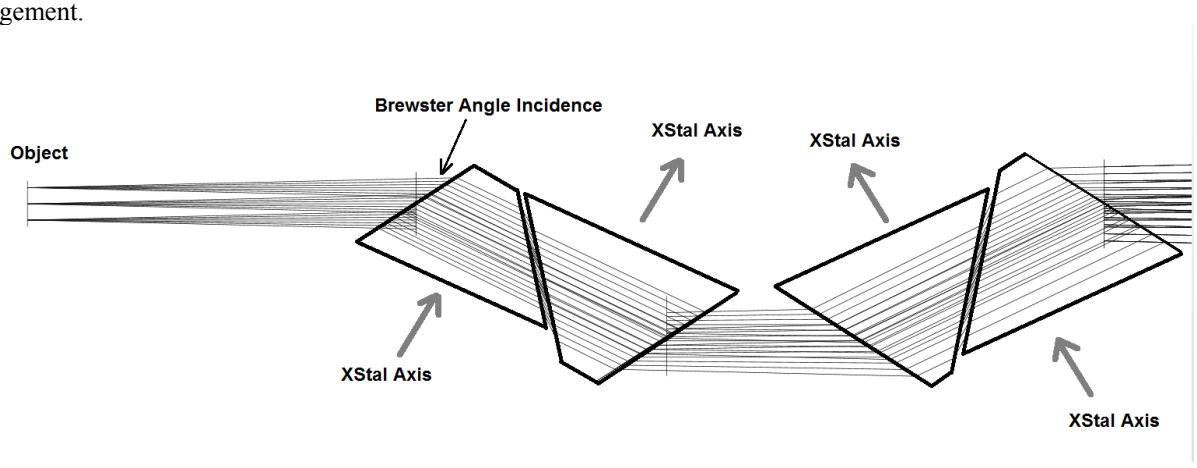

Figure 6: Modified Glan-Taylor polarising prism arrangement. All four prisms are made from barium borate.

Choice of barium borate as the prism material is dictated by the high level of birefringence and good transmission for the whole instrument wavelength range, particularly the ultraviolet.

3.3 Lenses

The pupil relay lens is a simple diverging plano-concave fused silica lens with a diameter of 12 mm and a nominal (@ 400 nm) focal length of -3000 mm. It is situated approximately 180 mm from the object location. The achromatic collimating lens consists of a fused silica, calcium fluoride pair with a diameter of approximately 90 mm. Their prescriptions are set out in Table 2.

Table 2: Prescriptions for collimating lens doublet. All figures are in mm.

	CaF2 'Crown' Lens		**Silica 'Flint' Lens**	
	Surface 1	Surface 2	Surface 1	Surface 2
Radius	Infinity	-193.39	-189.02	-636.80
Focal Length	411		-608	
Diameter	100		100	
Thickness	12		12	

The focal length of the lens elements in Table 2 are broadly in line with the simple analysis. In fact, the values are slightly smaller to compensate for the diverging effects of the pupil relay lens.

3.4 Mechanical

The whole crystal/ lens assembly is to be implemented as a tube mounted system. To rotate the direction of polarisation, the whole assembly is rotated bodily on bearings mounted at either of the tube. This arrangement, by virtue of its symmetry, reduces the tendency for misalignments to impact the transmission during rotation. It is imperative that misalignments and other geometrical effects do not modify module transmission over the 360° rotation of the module. Naturally, it is important that all components are accurately aligned with respect to the axis of rotation of the module. Nowhere is this more significant than in the alignment of the polarising crystals. Any systematic change in the output flux during rotation should be kept to less than 1 part in 10^3 and any residual effect should be reproducible and known to 1 part in 10^4.

The mechanical design is centred around an extruded aluminium rail which is fixed to an optical breadboard. There are four main subassemblies which referenced against, and affix to the breadboard. The integrating sphere is a hollow sintered PTFE clamshell in an aluminium box on a base, which can be adjusted in x and y by moving a plate using fine pitch adjuster screws. The second subassembly in the optical path is the condensing lens and object target. These are each held in their own mount, cantilevered inside the rotation stage using of four steel rods.

The third subassembly comprises of the rotation mount fixed to a bracket, and a cup-shaped component which interfaces to the bracket with a high-precision bearing. Between the bearing within the rotation stage itself and the precision bearing placed a prescribed distance away from the rotation stage, the cup will constrain its components (polarising crystal, silica flats and pupil lens) to the required axial tolerance.

The final subassembly uses two precision bearings, to constrain a doublet lens (in this case, mounted on a length of tube), and to rotate as required. The rotation of the fourth subassembly is entirely dictated by the position of the rotation stage because the rotational translation is transferred by means of a long aluminium tube with two coaxial dowels on each end. These dowels fit loosely within corresponding slots in the rotating components of the subassemblies, and are held firmly to one edge of it using tension springs. In this way, the angular position is conveyed absolutely, while avoiding over-constraining the system. The arrangement is shown in Figure 7.

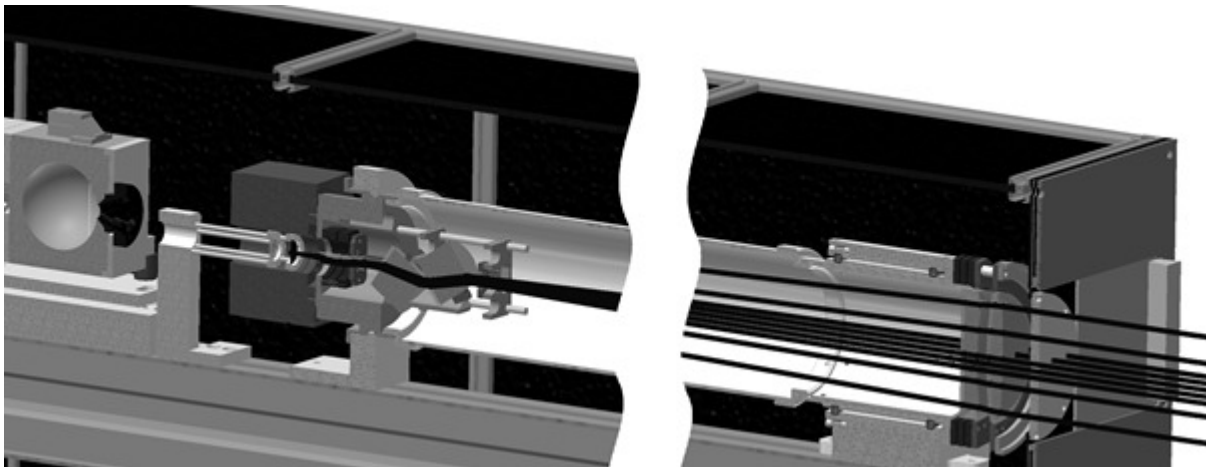

Figure 7: Mechanical arrangement of polariser. The integrating sphere shell is on the left with the prism/optical flat toward the centre. On the right is the doublet lens – close to the rotary bearing

4 MODELLED PERFORMANCE

4.1 Wavefront Error

The wavefront error performance is dominated by two factors. Firstly, as previously suggested, because of the very broad operating range, there is likely to be a significant amount of 'secondary colour' present. In addition, however, the introduction of tilted polarising prisms (at the Brewster angle) introduces astigmatism which is corrected by the tilted silica flats. In reality, correction can only be applied absolutely at one wavelength. That is to say, this astigmatism itself has a chromatic element. Nevertheless, the wavefront error is within the 150 nm requirement, except at the extreme margins. This is illustrated in Figure 8.

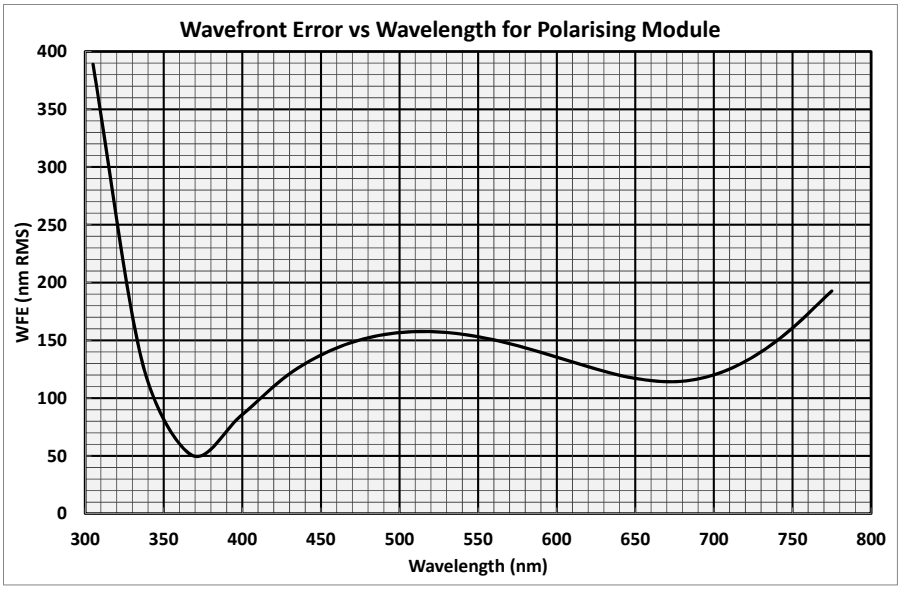

Figure 8: Wavefront error vs. wavelength for Polarising module. Note the two minima – these represent the two optimisation wavelengths for the 'achromatic' design. The residual background wavefront error is due to uncorrected (chromatic) astigmatism.

4.2 Pupil Uniformity

The symmetric crystal design, with two polarising crystal blocks instead of one, significantly reduces the variation in transmission as a function of numerical aperture. Some of the extra-ordinary ray is reflected internally, and this Fresnel reflection depends significantly upon the incidence angle. However, the effect on non-uniformity is smaller with the proposed arrangement and also symmetrical about the chief ray. The variation in throughput versus angle is greatest at the short uv wavelengths and this is illustrated in Figure 9 which shows a plot of uniformity against wavelength.

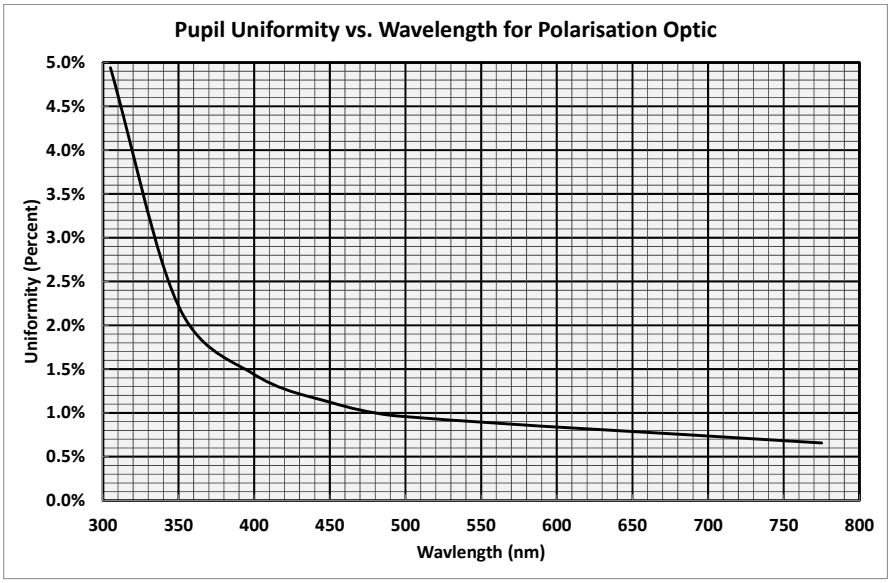

Figure 9: Pupil Uniformity vs. wavelength for polarising module.

4.3 Tolerancing

The tolerance analysis was performed twice, once using the beam illumination non-uniformity specification (<10%) as the criterion for optimisation. Secondly, optimisation was carried out based on the wavefront error specification (less than 150 nm rms). The final tolerances satisfy both cases. The analysis was performed considering tolerances associated with manufacturing, assembly and alignment.

The shape error used for the collimation lenses was 150 nm rms per surface equivalent to a transmitted wavefront error of λ/6 nm rms or λ/2 ptv. For prisms and cylinders a shape error of λ/4 nm rms was used. Standard tolerances are assumed for the rest of parameters: ± 0.001 for tolerance on the index of refraction, ± 0.1 mm for decentre, ± 0.1 mm for tolerances on thickness and ± 5 arc min for tolerances on tilts or wedges. The crystals sub-system is critically adjusted so tolerances are very tight and a high accuracy is required. Angles on the crystals are tightly specified, since a relatively small shift in incidence angle would substantially impact pupil uniformity. The tilt angle about Y axis for the pack of the four prisms has been considered as a compensator. This is the only compensator with a real impact in the final result. Application of this compensator improves the final result and the range of adjustment required is ± 1.65˚.

4.4 Straylight

For the stray light analysis, a non-sequential model of the Polariser Module was generated, as shown in Figure 10. This included, not only the optical surfaces themselves and mounting hardware, but also the system baseplate and enclosure. Characterisation of the disposition of the straylight is an essential part of the instrument calibration process. To model the characteristics of the instrument itself, a paraxial lens has been added at the pupil position to focus the beam on the detector and evaluate the incoherent irradiance at the image plane. All non-optical surfaces have been modelled as scattering surfaces with a Lambertian scatter fraction of 3%.

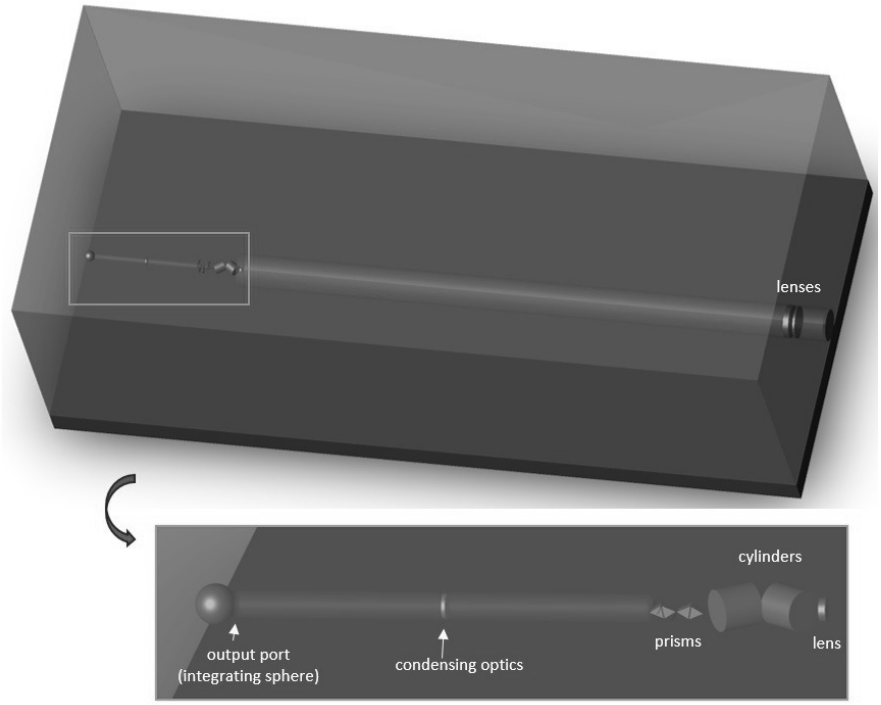

Figure 10: Non-sequential model of the Polariser Module.

The analysis revealed that that the stray light contribution attributed to cleanliness, mainly dust deposited over the optical surfaces was not likely to be significant compared to the scattering contribution from the mirrors and is not considered further here. A conservative cleanliness level of 200 as per MIL-STD-1246C was modelled[4,5].

Scattered light and ghosts were analysed individually. The scattered light was evaluated for two different cases, one of them for a point source and the second case considering a Lambertian circular source corresponding to the output port of the integrating sphere and coupling the condensing optics lens to the layout. In both cases, the scattered light obtained was negligible, so the only significant source of stray light in the polariser module corresponds to ghosts generated by reflection at the interface of refractive surface. Initial analysis had suggested that the (conventional) Glan-Taylor prism arrangement would produce a significant ghost between the two input and output faces of the prism. In this arrangement, the two faces are parallel, and the residual reflection from these faces would give rise to a significant ghost. This has been circumvented with the current design, in that the prisms do not contribute to the ghosting. Firstly, the input and output faces of the prisms are at the Brewster angle, so the residual reflection for the extra-ordinary ray is insignificant. Secondly, any residual reflection at the polarising facet is lost by exiting the prism, as per the ordinary ray.

With the amelioration of the polariser ghost, it is the 3 lenses and the test chamber window that make any significant contribution to the ghosting. 'Lens 1' is the small pupil imaging lens, 'Lens2' is the first (silica) of the two doublet elements and 'Lens3' is the final (CaF_2) doublet element. The worst offender is the test chamber window, as seen in Figure 1, with the double Fresnel reflection producing an irradiance of 0.13% of that of the nominal image. The wedge of this window is specified to be between 36 and 72 arc seconds, producing a ghost reflection between 1.2 and 2.4 arcminutes from the main image. The size of the image is 4 arc minutes, so the ghost image will not have been displaced away from the main image. The next most serious ghost arises from the pupil imaging silica lens (Lens 1). From the perspective of ghosting, this lens needs to be placed relatively far from the object. However, this restriction would further compromise the optimisation of the wavefront error. The particular concern here is the degradation in the uniformity of the 4 x 4 arcminute field of view. More specifically, the ghosting may impact the stability of the 45

arcsecond sub-field illumination when the beam deviates by ±1 arcminute. The pupil imaging lens produces a defocussed ghost 1.36 minutes in diameter that is aligned to the main image.

From the perspective of the overall system requirements, these ghosts should not produce a flux deviation of greater than 0.01% over a 45 arcsecond sub-field of the image. For the pupil imaging lens, this effect would only be produced if there is a beam deviation of greater than 1.4 minutes, which is considerably greater than the requirement (1 min). Essentially this ghost produces a mild shadowing effect at the edges of the 4 x 4 minute image; this is not accessed by 45 arc second subfield under any reasonable conditions. The situation is different for the window ghosts. Here, a 'sharp' edge is introduced anywhere between the centre and 0.8 arc min from the centre. This edge introduces a non-uniformity and, in order to eliminate it, the TV window wedge should either be less than 18 arc seconds or greater than 102 arcseconds. Other ghosts do not contribute significantly.

5 CONCLUSIONS

A polarising module designed to produce highly uniform collimated light with well characterised linear polarisation to a satellite based imaging spectrometer has been described. The polarising module is to be used as part of the calibration programme for the satellite instrument. A novel polarising device has been devised that is based upon a Glan-Taylor arrangement and provides highly uniform linearly polarised light in a moderately diverging beam. The performance, including wavefront error and straylight characteristics have been described in detail.

6 ACKNOWLEDGEMENTS

The authors acknowledge the European Union, the European Space Agency, EUMETSAT, Airbus DS and Mullard Space Science Laboratory. This document has been produced with the financial assistance of the European Union. The views expressed herein can in no way be taken to reflect the official opinion of the European Union and/or ESA. The authors also wish to thank Dr. J.F. Pittet of Airbus DS for helpful discussions.

6 REFERENCES

[1] Bazalgette Courrèges-Lacoste, G., Ahlers, B., Guldimann, B., Short, A., Veihelmann, B. and Stark, H., "The Sentinel4/UVN instrument on-board MTG-S", Proc. EUMETSAT Meteorological Satellite Conf., 5–9 September 2011, Oslo, Norway, p. 59 (2011)

[2] Noëll, S., Bramstedt, K., Bovensmann, H., Gerilowski, K., Burrows, J. P., Standfuss, C., Dufour, E. and Veihelmann, B., "Quantification and mitigation of the impact of scene inhomogeneity on Sentinel-4 UVN UV-VIS retrievals", Atmos. Meas. Tech., **5**, 1319–1331, (2012)

[3] Archard, J.F.; Taylor, A.M. (1948). "Improved Glan-Foucault prism". J. Sci. Instrum. **25**, 407–409, (1948)

[4] MIL-STD-1246, "Military standard product cleanliness and contamination control program", US Department of Defense, (1991)

[5]: Peterson, R. V., Magallanes, P. G., Rock, D. F., "Tailored Particle Distributions Derived from MIL-STD-1246". Proc. SPIE, Vol. 4774: Optical System Contamination: Effects, Measurements, and Control VII (2002).